FEBS Letters 491 (2001) 174–179 FEBS 24625

Crystal structure of the oxidized cytochrome c_2 from *Blastochloris viridis*

Satoshi Sogabe[a,1], Kunio Miki[b,c,*]

[a] *Research Laboratory of Resources Utilization, Tokyo Institute of Technology, 4259 Nagatsuta, Yokohama, Kanagawa 226, Japan*
[b] *Department of Chemistry, Graduate School of Science, Kyoto University, Sakyo-ku, Kyoto 606-8502, Japan*
[c] *RIKEN Harima Institute/SPring-8, Koto 1-1-1, Mikazukicho, Sayo-gun, Hyogo 679-5148, Japan*

Received 16 October 2000; revised 14 January 2001; accepted 22 January 2001

First published online 9 February 2001

Edited by Richard Cogdell

Abstract The crystal structure of the oxidized cytochrome c_2 from *Blastochloris* (formerly *Rhodopseudomonas*) *viridis* was determined at 1.9 Å resolution. Structural comparison with the reduced form revealed significant structural changes according to the oxidation state of the heme iron. Slight perturbation of the polypeptide chain backbone was observed, and the secondary structure and the hydrogen patterns between main-chain atoms were retained. The oxidation state-dependent conformational shifts were localized in the vicinity of the methionine ligand side and the propionate group of the heme. The conserved segment of the polypeptide chain in cytochrome *c* and cytochrome c_2 exhibited some degree of mobility, interacting with the heme iron atom by the hydrogen bond network. These results indicate that the movement of the internal water molecule conserved in various *c*-type cytochromes drives the adjustments of side-chain atoms of nearby residue, and the segmental temperature factor changes along the polypeptide chain. **© 2001 Federation of European Biochemical Societies. Published by Elsevier Science B.V. All rights reserved.**

Key words: Cytochrome c_2; Oxidation state; Crystal structure; Electron transfer

1. Introduction

c-Type cytochrome is one of the best-characterized electron transport proteins. However, the nature and role of the oxidation state-dependent conformational changes leading to the biological electron transfer reaction remain to be clarified. Studies using techniques such as nuclear magnetic resonance (NMR) analysis [1] and the hydrogen exchange rates method [2] have indicated that the protein undergoes dramatic conformational changes upon a change of oxidation state. On the other hand, other studies have suggested that the conformational differences between the reduced and oxidized forms are very small [3].

Bacterial cytochrome c_2 serves as the bacterial counterpart of eukaryotic cytochrome *c* and generally functions as a water-soluble electron carrier between membrane-bound redox centers in biological processes such as photosynthesis and respiration [4]. The physiological function of cytochrome c_2 is to transfer electrons from ubiquinol-cytochrome *c* oxidoreductase (the cytochrome bc_1 complex) to the photosynthetic reaction center (RC) in order to reduce the photo-oxidized bacteriochlorophyll dimer, which is the primary electron donor in the RC [5].

Oxidation state-coupling conformational changes in eukaryotic cytochrome *c* have been well characterized. Structural studies on yeast iso-1-cytochrome *c* [6,7] have suggested that subtle structural changes occur between both oxidation states, and that the internally bound water molecule involved in the hydrogen bond network plays an important role in triggering the subsequent conformational changes [8]. A tyrosine residue involved in the hydrogen bond network with the heme iron has been studied using a variety of techniques, such as semi-synthesis [9] and site-directed mutagenesis [10]. Further structural studies of specifically mutated cytochromes *c* have also provided evidence that the function of the hydrogen bond network is dependent on the oxidation state [11,12].

To date, the structures of cytochrome c_2 from *Rhodospirillum rubrum* [13], *Rhodobacter capsulatus* [14], *Rhodobacter sphaeroides* [15], *Blastochloris viridis* [16], *Rhodopila globiformis* [17], and *Paracoccus denitrificans* [18] have been reported. The solution structure for cytochrome c_2 from *R. capsulatus* has also been reported in an investigation on backbone dynamics and conformational flexibility [19]. However, no structural comparison between two oxidation states for cytochrome c_2 has been investigated, while the structural differences between the two redox forms of cytochrome *c* have been detected by NMR spectroscopy [20–22] and X-ray crystallography [8].

We have solved the crystal structure of *B. viridis* cytochrome c_2 in oxidized form in order to better understand the oxidation state-dependent structural alternations. We describe here the conformational changes in the polypeptide chain backbone between the two oxidation states, which are associated with the changes of segmental temperature factors. Our results suggest that the internally bound water molecule may play an important role in the oxidation state-dependent conformational changes in the hydrogen bond network involving the methionine heme ligand. Consequently, the results of this study should provide considerable insight into the mechanism of electron transfer in the bacterial cytochrome c_2.

2. Materials and methods

2.1. Crystallization and data collection

The reduced form of *B. viridis* cytochrome c_2 was purified and crystallized in the reduced form as previously described [23]. In order to obtain crystals of the oxidized form, crystals of the reduced form

*Corresponding author. Fax: (81)-75-753 4032.
E-mail: miki@kuchem.kyoto-u.ac.jp

[1] Present address: Nippon Roche Research Center, 200 Kajiwara, Kamakura, Kanagawa 247-8530, Japan.

Abbreviations: RC, reaction center

0014-5793/01/$20.00 © 2001 Federation of European Biochemical Societies. Published by Elsevier Science B.V. All rights reserved.
PII: S0014-5793(01)02179-2

were soaked for 2 h in a mother-liquor solution containing 40 mM potassium ferri-cyanide as oxidant prior to the mounting for diffraction studies. From the optical absorption spectra of solubilized crystals soaked in oxidant, it was confirmed that cytochrome c_2 was in its oxidized form. The crystals retained their diffraction quality despite soaking. Crystals of the oxidized form were isomorphous with those of the reduced form, and the unit-cell dimensions were $a = b = 75.97$ Å and $c = 40.37$ Å. Intensity data of crystals of the oxidized form as well as those of the reduced form were collected with synchrotron radiation at the BL-6A beam line of the Photon Factory, the National Laboratory for High Energy Physics, Tsukuba, Japan [16]. The crystals were stable towards X-ray exposure and the diffraction was recorded beyond 1.9 Å resolution. Intensity data were evaluated by the program WEIS [24] and processed by the program package PROTEIN [25]. A total of 10 094 independent reflections were obtained after scaling and merging of 38 974 measurements with the merging R-value of 0.068 at 1.9 Å resolution, which corresponds to 93.2% of the total theoretical number of observations.

2.2. Structure refinement

The structure of *B. viridis* cytochrome c_2 in the oxidized form was refined using the structure of the reduced form as a starting model [16] by the program X-PLOR [26]. Before refining the structure of the oxidized form, an 'oxidized-minus-reduced cytochrome c_2' difference Fourier map was calculated. This electron density map indicated that no large positional shifts of the polypeptide chain were present between the two oxidation states. The refinement was performed using the diffraction data in the resolution range of 15.0–1.9 Å with bulk-solvent correction. The model was made successively through systematic inspection of simulated-annealing omit maps using the program O [27]. Well ordered water molecules were included in the refinement model in cases in which electron density peaks were situated so as to provide at least one appropriate hydrogen bond to protein atoms or other water molecules. In order to compare between two redox forms without bias, the structure of the reduced form was also refined in the same algorithm. The coordinates of the structure will be deposited in the Protein Data Bank under accession number 1IO3 (http://ww.rcsb.org/pdb/).

3. Results and discussion

3.1. Quality of the model

The refined structure of the oxidized *B. viridis* cytochrome c_2 has nearly ideal stereochemistry, and its crystallographic R-factor and free-R are 20.8% and 24.3% at 1.9 Å resolution, respectively. The structure contains all of the 107 amino acid residues, one heme prosthetic group and 42 water molecules. The bond deviation and angle deviation of the model are 0.076 Å and 2.95°, respectively. From the Luzzati plots [28], the positional errors are estimated to be below 0.25 Å for the model. Compared with the structure of the reduced form, that of the oxidized form showed some disordered residues with higher temperature factors (see below). The overall average temperature factors were comparable between the two oxidation states for all atoms in the polypeptide chain (20.3 Å^2 and 23.1 Å^2 in the reduced and oxidized form, respectively).

3.2. Overall structure

The polypeptide folding is composed of five α-helical elements, one reversed γ-turn, one type I β-turn and six type II β-turns folding a roughly globular shape and forming a heme binding pocket (Fig. 1). The root-mean-square positional deviations and the temperature factor differences between corresponding main-chain and side-chain atoms of the two redox forms are shown in Fig. 2. The observed conformational changes of the backbone fold were small, and it is noteworthy that the hydrogen bond interactions between main-chain atoms were retained upon the change of oxidation state. The overall average value for main-chain atom differences for all residues was 0.15 Å. The difference observed in the N-terminus was probably due to differential fits to the poor electron density in this region rather than a change of the oxidation state.

Some regions of the polypeptide chain showed conformational changes resulting from the difference in oxidation state. One region involved the pyrrole ring A propionate group and its surrounding residues. The differences in residues 42–44 result in the positional shift of the side chain of Tyr 47, which forms a hydrogen bond with this heme propionate. The additional conformational changes around the main chain of Asn 51 and Trp 58 were probably due to removal or weakening of the hydrogen bond between these residues and the heme propionate in the oxidized form (see below). Other large displacements of side chains were due to poorly defined residues on the molecular surface, e.g. lysine and glutamate, and appeared to result from their higher degree of mobility and higher temperature factors rather than from the change of oxidation state.

The temperature factor fluctuation was substantially different between the two oxidation states. In the oxidized form, the residues 69–81 have the higher temperature factors with a maximal increase for Lys 78 (Fig. 2B). Furthermore, residues 74–77 compose a type II β-turn, involving Thr 77 composed of the hydrogen bond network with the internally bound water molecule (Wat 1: Fig. 1). This water molecule showed a large shift dependent on the oxidation state of the heme iron. The structure of *R. sphaeroides* cytochrome c_2 complexed with an imidazole revealed that this segment exhibited considerable flexibility and was involved in a conformational change leading to breakage of the iron–methionine bond by imidazole binding [15]. That the oxidized form shows greater polypeptide chain flexibility has also been suggested by studies using NMR [29] and X-ray scattering [30].

The heme group is almost completely buried within a hydrophobic pocket formed by the polypeptide chain. Total

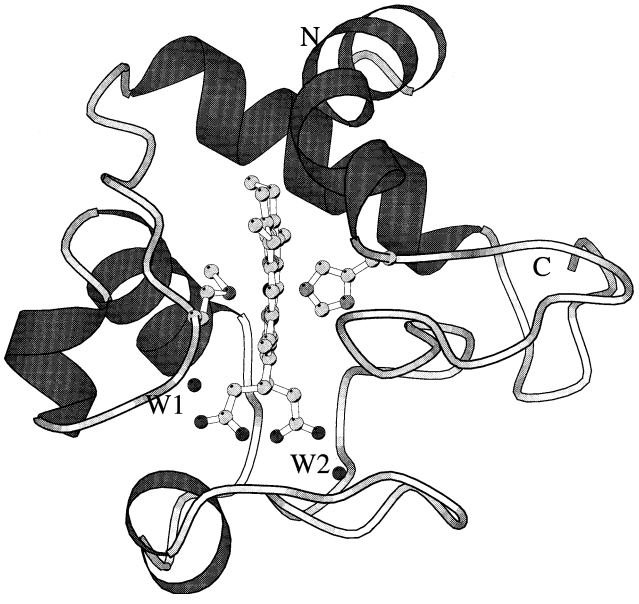

Fig. 1. Ribbon diagram of the structure of the oxidized *B. viridis* cytochrome c_2. Two water molecules (Wat 1 and Wat 2) in the vicinity of the heme are also shown. This figure was prepared with MOLSCRIPT [33].

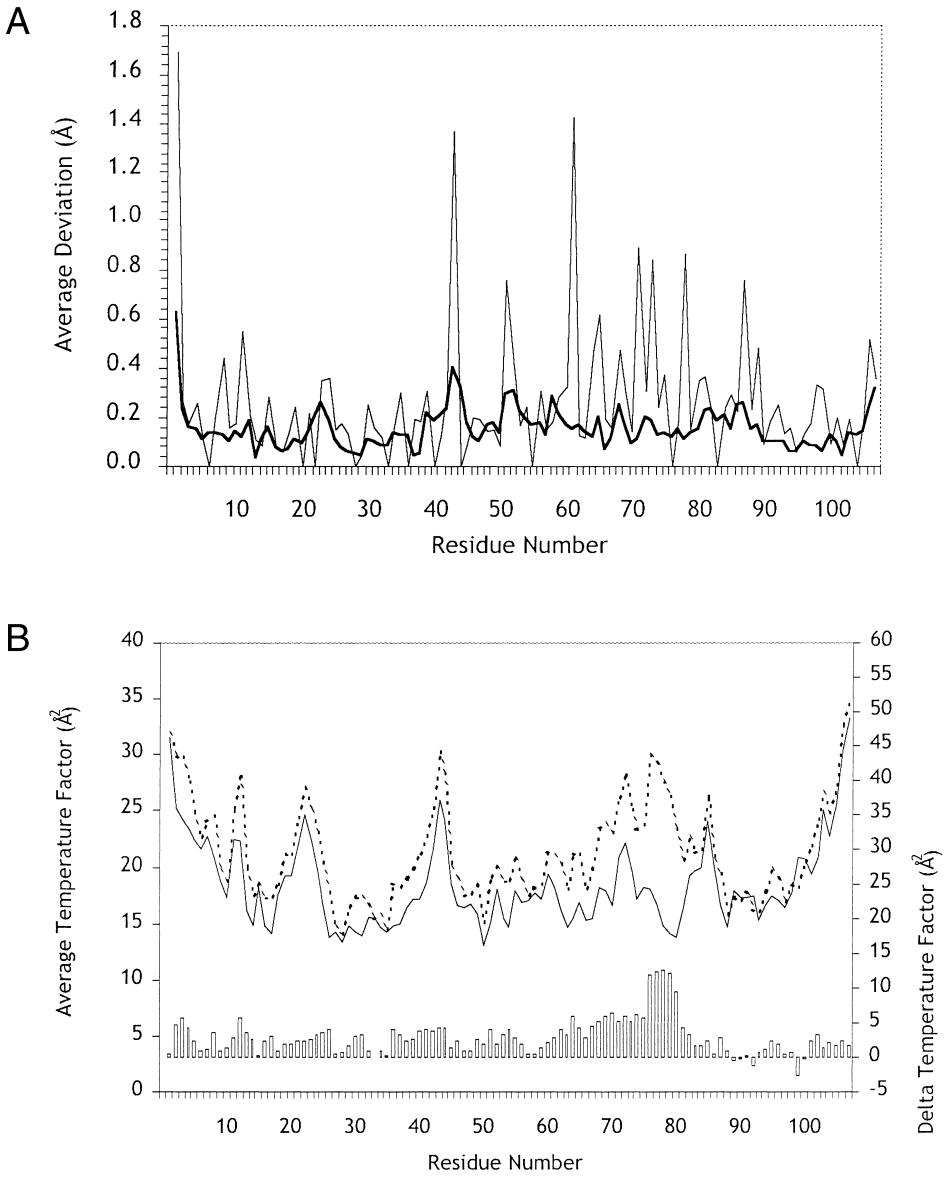

Fig. 2. (A) Root-mean-square positional deviations between two redox forms of main-chain (thick lines) and side-chain (thin lines) atoms per residues. (B) Average temperature factors per residue for the reduced (solid lines) and oxidized (dot lines) forms. The differences of the temperature factors between the two oxidation states are shown in the bar graph in the lower panel.

heme solvent accessibility is comparable between the two oxidation states. The exposed solvent area of the heme group is 6.0% and 6.3% for the reduced and oxidized form, respectively. The degree of exposure is similar to those calculated in other *c*-type cytochromes [8]. On the other hand, the solution structures of cytochrome *c* showed that the surface area of the reduced heme accessible to the solvent is smaller than that of the oxidized form due to displacement of the residues which surround the exposed heme edge [20]. The opening of the heme crevice upon oxidation and the resulting increase in solvent accessibility of heme propionates could account for the difference of free energy between the two oxidation states [31].

3.3. Heme and iron coordination

In both the reduced and oxidized forms, the porphyrin rings of the heme group are similarly distorted from planarity into a saddle shape. Bond distances for the heme iron coordination are not significantly different between the two oxidation states, although a slight deviation is observed for the heme axial ligand. These results are in good agreement with those from a previous structural comparison between the structures of yeast iso-1-cytochrome *c* in each of the two oxidation states [8]. This suggests that the heme conformation and the heme iron coordination may be independent of the oxidation state. It is notable that an increase in the average temperature factor for the side chain of Met 79 is observed on changing from the reduced to the oxidized form (from 14 Å^2 to 26 Å^2), although the average displacement of the side-chain atoms is within the range of experimental error. With respect to the differences in temperature factors, it might be suggested that the Met 79 SD–heme iron ligand bond is sensitive to the change of the oxidation state. In contrast, the ligand-bond distance and temperature factors for His 17 are comparable between the two oxidation states.

As described above, the structural differences between the

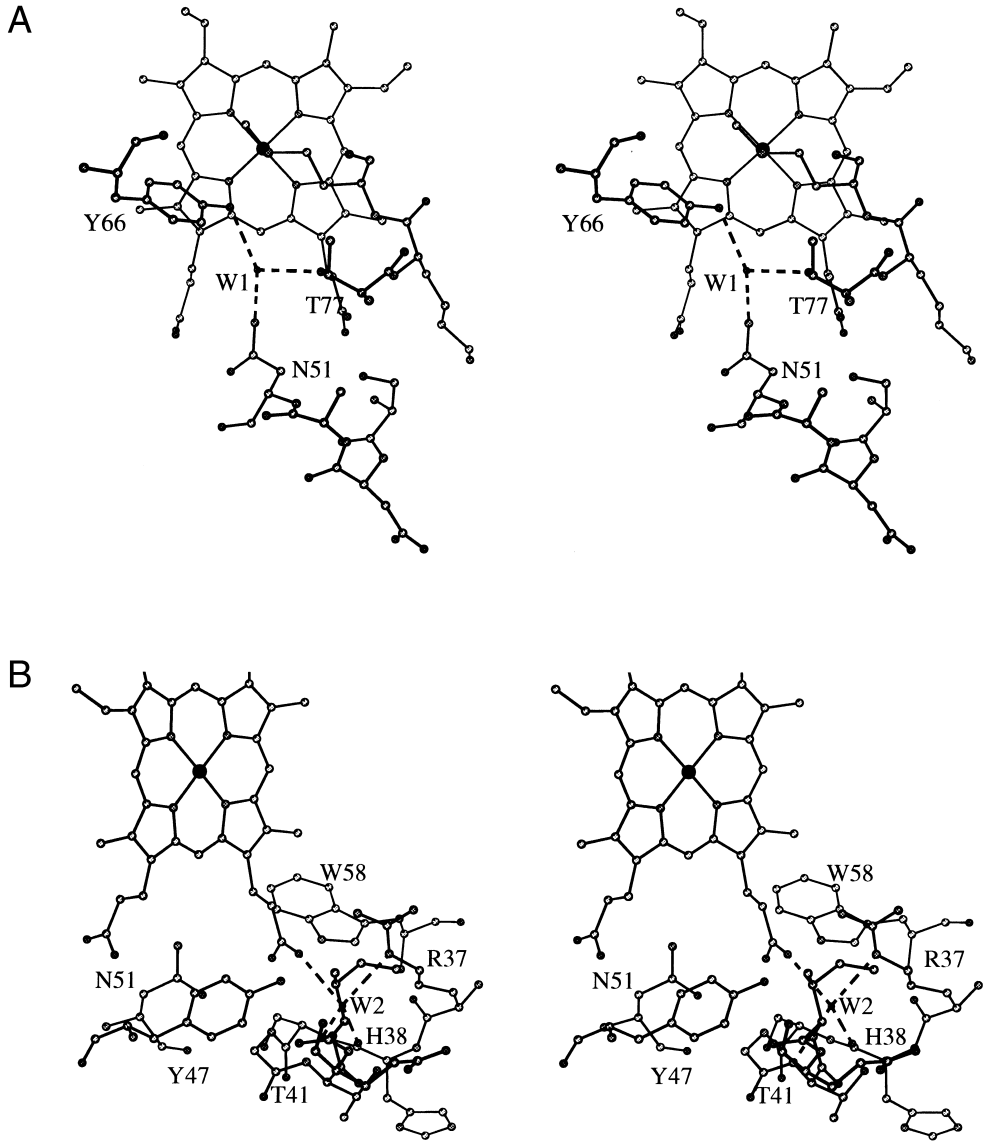

Fig. 3. Local environments of the internal water molecules and their hydrogen bond interactions with the heme and the surrounding amino acid residues. (A) Wat 1 and (B) Wat 2. Hydrogen bonds are shown with broken lines. This figure was prepared with MOLSCRIPT [33].

two oxidation states are located around the pyrrole ring A propionate. The residues that form the hydrogen bond with this propionate can accommodate the positional shifts upon a change of the oxidation state. These include interactions with Gly 40, Tyr 47, Asn 51 and Trp 58. The strength of the hydrogen bond was judged by the hydrogen bond distance and the temperature factor for the side chain of the residue. The slight rearrangement of this propionate leads to shifts in the main-chain and side-chain atoms of these residues, thereby weakening the hydrogen bond with Trp 58 and breaking the hydrogen bond with Asn 51. In addition, the positional deviations of the residues 42–44 are due to the shift in the side chain of Tyr 47. It is notable that these conformational changes are attributed to the higher temperature factors in the oxidized form, in association with the mobility of the polypeptide chain of the residues 40–52. In contrast, the hydrogen bond interaction between Asn 51 and this propionate is broken on changing from the reduced to the oxidized form. It has been suggested that both the localization of negative charge in the porphyrin ring and the electrostatic interaction of the propionate groups have an effect on the conformation [1]. Structural studies on mutants of yeast iso-1-cytochrome *c* [11,12] have suggested that the conformational changes around this propionate are driven by the shift in the side chain of Asn 52 (Asn 51 in *B. viridis* cytochrome c_2), along with the oxidation state-dependent movement of the internal water molecule (see below).

The temperature factor increase of Met 79 in the oxidized form may be accounted for by the weakness of the hydrogen bond between Tyr 66 OH and Met 79 SD (Fig. 2B). It is notable that the methionine heme ligand is involved in both the oxidation state-dependent changes and the movement of the internal water molecule (Wat 1; Fig. 3A). The movement of this water molecule, which is dependent on the oxidation state, would modulate the bond between the methionine ligand and the heme iron (see below).

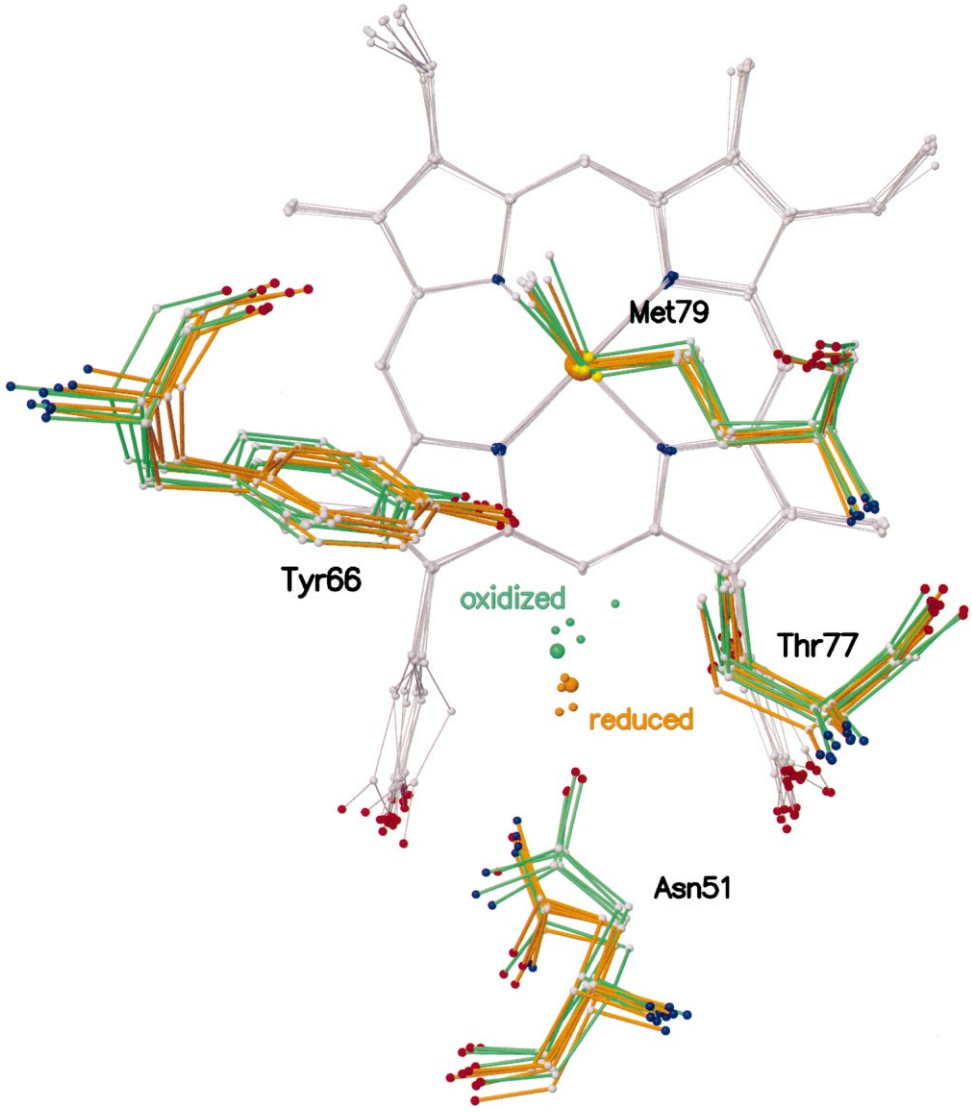

Fig. 4. Schematic drawing of the heme environment in *B. viridis* cytochromes c_2 from *B. viridis* and *R. globiformis* and eukaryotic cytochromes *c*. The positions of the water molecules are compared with those of reduced forms of cytochrome c_2 from *R. globiformis* (1HRO [17]) and cytochromes *c* from tuna (3CYT 5CYT [34]) and yeast (iso-1: 1YCC [6] and iso-2: 1YEA [35]), and oxidized cytochromes *c* from tuna (5CYT 3CYT [36]), rice (1CCR [37]), horse (1HRC [38]) and yeast (iso-1: 2YCC [7]). The water molecules and the amino acid residues involved in the hydrogen bond network (Asn 51, Tyr 66, Thr 77 and Met 79 in the sequence of *B. viridis*) in the reduced and oxidized forms are shown in orange and green, respectively. Among the water molecules in the oxidized and reduced forms, those of *B. viridis* cytochrome c_2 are depicted in larger ball models magenta and orange, while those of the others *c* are shown in purple and yellow smaller ones, respectively. This figure was created with MOLSCRIPT [33] and RASTER 3D [39].

3.4. Water molecules

It has been reported that *B. viridis* cytochrome c_2 shows greater homology to eukaryotic cytochromes *c* than to other cytochromes c_2 with respect to not only molecular folding but also two water molecules in the vicinity of the heme, which have been located at a common site in both eukaryotic cytochromes *c* and *B. viridis* cytochrome c_2 [16]. One of these molecules is Wat 1, which forms a hydrogen bond network with three buried residues (Asn 51 ND2, Tyr 66 OH and Thr 77 OG1), as shown in Fig. 3A. This hydrogen bond network in *B. viridis* cytochrome c_2 is different from that of other cytochromes c_2 [16]. The second water molecule is Wat 2, which forms hydrogen bonds with Arg 37, His 38, Thr 41 and the heme propionate (Fig. 3B). Wat 2 is positioned at almost the same site in both oxidation states and retained its interaction with the protein and heme. In eukaryotic cytochromes *c*, this water molecule forms a hydrogen bond to an oxygen atom of the propionate in the reduced form, while it is shifted and interacts with both the propionate carboxyl oxygen atoms in the oxidized form [7].

Wat 1 undergoes a subtle positional shift toward heme iron upon a change of oxidation state, as shown in Fig. 4. The side chain of Asn 51 to which Wat 1 forms a hydrogen bond is mostly affected by this movement, although there is no significant alteration in the main-chain conformation. The hydrogen bond between the side chain of Asn 51 and the pyrrole ring A propionate group is broken. The side chains of Tyr 66 and Thr 77 show little shift in positions, retaining the hydrogen bonds with Wat 1. Despite the retention of the hydrogen bond between Wat 1 and Thr 77, the main-chain atoms of the residues 74–81 exhibit the increased temperature factors in the oxidized form, so that this segment becomes substantially

more mobile. The temperature factors of Wat 1 are 27 and 19 Å^2 in the oxidized and reduced forms, respectively. This observation suggests that Wat 1 contributes to the increased mobility of nearby polypeptide chains in the oxidized form and may serve to change the oxidation state of the heme iron through alteration in the surrounding hydrogen bond network.

The positions of Wat 1 in both oxidation states in *B. viridis* cytochrome c_2 are almost superimposed with those of the eukaryotic cytochromes *c* (Fig. 4). In addition, the positional shift upon the change of the oxidation state occurs in a manner similar to that of eukaryotic cytochrome *c*. In mutants of yeast iso-1-cytochrome *c*, the hydrogen bond network involving the internal water molecule has been shown to increase the flexibility of polypeptide chains and destabilize the protein [32]. This water molecule is also conserved in *R. globiformis* cytochrome c_2, which belongs to the 'small' cytochrome c_2 subgroup [17]. The residues 70–85 are a highly conserved segment in 'small' cytochromes c_2 and cytochromes *c*, having a great degree of mobility (see above). It has been reported that this conserved segment acts as a switch for conformational changes between the two oxidation states to facilitate the electron transfer, and that these changes would be related to the interactions between cytochrome *c* and its redox partners [8]. These results suggest that this water molecule found in various *c*-type cytochromes plays an important role in adjusting the redox potential with alteration of the surrounding hydrogen bond network. This is also supported by the high cross-species conservation of these surrounding amino acid residues, to which this internal water molecule is hydrogen-bonded in eukaryotic cytochromes *c*. The positions of this water molecule in the crystal structures of the two redox forms are roughly similar to those in the solution structures of cytochrome *c* (data not shown).

Acknowledgements: The authors thank Dr. Masasuke Yoshida for his kind support, Miyako Miki for preparation of *B. viridis* cytochrome c_2, and Drs. Noriyoshi Sakabe, Atsushi Nakagawa and Nobuhisa Watanabe of the Photon Factory, Japan, for their help in data collection using synchrotron radiation. This work was performed under the approval of the Photon Factory Advisory Committee (proposal No. 93G065) and the authors are members of the Sakabe Project of TARA (Tsukuba Advanced Research Alliance). This work was supported in part by Grants-in-Aid for Scientific Research on Priority Areas (Nos. 03241103, 04225103, 04266208 and 05244102) to K.M. and also by a Kurata Research Grant from the Kurata Foundation to K.M.

References

[1] Moore, G.R. (1983) FEBS Lett. 161, 171–175.
[2] Liu, G., Crygon, C.A. and Spiro, T.G. (1989) Biochemistry 28, 5046–5050.
[3] Feng, Y., Roder, H. and Englander, S.W. (1990) Biochemistry 29, 3494–3504.
[4] Bartsch, R.G. (1978) in: Cytochromes (Clayton, R.K. and Sistrom, W.R., Eds.), pp. 249–279, Plenum, New York.
[5] Michel, H. and Deisenhofer, J. (1986) in: Encyclopedia of Plant Physiology (Staehelin, A.C. and Arntzen, C.J., Eds.), pp. 371–381, Springer, Berlin.
[6] Louie, G.V. and Brayer, G.D. (1990) J. Mol. Biol. 214, 527–555.
[7] Berghuis, A.M. and Brayer, G.D. (1992) J. Mol. Biol. 223, 959–976.
[8] Brayer, G.D. and Murphy, M.E.P. (1996) in: Cytochrome *c* (Scott, R.A. and Mauk, A.G., Eds.), pp. 103–166, University Science Books, CA.
[9] Wallance, C.J.A., Mascagni, P., Chait, B.T., Collawn, J.F., Paterson, Y., Proudfoot, A.E. and Kent, S.B.H. (1989) J. Biol. Chem. 264, 15199–15209.
[10] Schejter, A., Luntz, T.L., Koshy, T.I. and Margoliash, E. (1992) Biochemistry 31, 8336–8343.
[11] Berghuis, A.M., Guillemette, J.G., Smith, M. and Brayer, G.D. (1994) J. Mol. Biol. 235, 1326–1341.
[12] Berghuis, A.M., Guillemette, J.G., McLendon, G., Sherman, F., Smith, M. and Brauer, G.D. (1994) J. Mol. Biol. 236, 786–799.
[13] Bhatia, G.E. (1981) in: Ph.D. Thesis, University of California, San Diego, CA.
[14] Benning, M.M., Wesenberg, G., Caffrey, M.S., Bartsch, R.G., Meyer, T.E. and Cusanovich, M.A. (1991) J. Mol. Biol. 220, 673–685.
[15] Axelrod, H.L., Feher, G., Allen, J.P., Chirino, A.J., Day, M.W., Hsu, B.T. and Rees, D.C. (1994) Acta Crystallogr. D 50, 596–602.
[16] Sogabe, S. and Miki, K. (1995) J. Mol. Biol. 252, 235–247.
[17] Benning, M.M., Meyer, T.E. and Holden, H.M. (1996) Arch. Biochem. Biophys. 33, 338–348.
[18] Benning, M.M., Meyer, T.E. and Holden, H.M. (1994) Arch. Biochem. Biophys. 310, 460–466.
[19] Cordier, F., Caffrey, M., Brutscher, B., Cusanovich, M.A., Marion, D. and Blackledge, M. (1998) J. Mol. Biol. 281, 341–361.
[20] Qi, P.X., Beckman, R.A. and Wand, A.J. (1996) Biochemistry 35, 12275–12286.
[21] Bertini, I., Dalvit, C., Huber, J.G., Luchinat, C. and Piccioi, M. (1997) FEBS Lett. 415, 45–48.
[22] Banci, L., Berniti, I., Huber, J.G., Spyroulias, G.A. and Turano, P. (1999) J. Biol. Inorg. Chem. 4, 21–31.
[23] Miki, K., Saeda, M., Masaki, K., Kasai, N., Miki, M. and Hayashi, K. (1986) J. Mol. Biol. 191, 579–580.
[24] Higashi, T. (1989) J. Appl. Crystallogr. 22, 9–18.
[25] Steigemann, W. (1992) PROTEIN, Max-Planck Institut fur Biochemie, Martinsried.
[26] Brunger, A.T. (1992) X-PLOR 3.1, Yale University Press, London.
[27] Jones, T.A. and Thirup, S. (1986) EMBO J. 5, 819–822.
[28] Luzzati, P.V. (1952) Acta Crystallogr. 5, 802–810.
[29] Williams, G., Clayden, N.J., Moore, G.R. and Williams, R.J.P. (1985) J. Mol. Biol. 183, 447–460.
[30] Trewhell, J., Carlson, V.A.P., Curtis, E.H. and Heidorn, D.B. (1988) Biochemistry 27, 1121–1125.
[31] Battistuzzi, G., Borsari, M., Sola, M. and Francia, F. (1997) Biochemistry 36, 16247–16258.
[32] Hickey, D.R., Berghuis, A.M., Lanford, G., Jaeger, J.A., Cardillo, T.S., McLendon, D., Das, G., Sherman, F., Brayer, G.D. and McLendon, G. (1991) Biochemistry 266, 11686–11694.
[33] Kraulis, P.J. (1991) J. Appl. Crystallogr. 24, 946–950.
[34] Takano, T. and Dickerson, R.E. (1981) J. Mol. Biol. 153, 79–94.
[35] Murphy, M.E., Nall, B.T. and Brayer, G.D. (1992) J. Mol. Biol. 227, 160–176.
[36] Takano, T. and Dickerson, R.E. (1977) J. Mol. Biol. 153, 95–115.
[37] Ochi, H., Hata, Y., Tanaka, N., Kakudo, M., Sakurai, T., Aihara, S. and Morita, Y. (1983) J. Mol. Biol. 166, 407–418.
[38] Bushnell, G.W., Louie, G.V. and Brayer, G.D. (1990) J. Mol. Biol. 214, 585–595.
[39] Merritt, E.A. and Murphy, M.E.P. (1994) Acta Crystallogr. D50, 869–873.